

The Atomic Superfluid Quantum Interference Device with tunable Josephson Junctions

Jiatao Tan¹ and Boyang Liu^{1,*}

¹*Institute of Theoretical Physics, School of Physics and Optoelectronic Engineering,
Beijing University of Technology, Beijing, 100124, China*

(Dated: November 27, 2024)

The atomic superfluid quantum interference device (ASQUID) with tunable Josephson junctions is theoretically investigated. ASQUID is a device that can be used for the detection of rotation. In this work we establish an analytical theory for the ASQUID using the tunneling Hamiltonian method and find two physical quantities that can be used for the rotation sensing. The first one is the critical population bias, which characterizes the transition between the self-trapping and the Josephson oscillation regimes and demonstrates a periodic modulation behavior due to the rotation of the system. We discuss the variation of critical population bias when the tunneling strengths of the junctions are tuned in different values, and find that the symmetric junctions are better choice than the asymmetric ones in terms of rotation sensing. Furthermore, how the initial phase difference between the two condensates affects the measurement of rotation is also discussed. Finally, we investigate the case of time-dependent junctions and find there is another physical quantity, named critical time, that can be used to detect the rotation.

I. INTRODUCTION

Atomtronics[1, 2] is an emerging field in quantum technology, focusing on the manipulation and control of ultracold atoms to create devices analogous to conventional electronics. Atomtronics utilizes neutral atoms in optical lattices or magnetic traps to form circuits, devices, and systems with unique quantum properties. In the field of quantum sensing the SQUID is widely used for measuring extremely weak magnetic fields [3]. Inspired by the applications of SQUIDs, the development of their atomic counterparts, ASQUIDs, attracts a lot of attention and opens up new possibilities for precision measurement [4–8]. The major difference between SQUID and ASQUID is that the superfluids in ASQUIDs are made of neutral atoms instead of Cooper pairs. Therefore, the ASQUID doesn't couple to the electro-magnetic fields. The phase twist of the condensates in ASQUID can be created by the physical rotation of the device, so ASQUID can be used for rotation sensing. With the advantages of high controllability and detection of atom number and phase of condensates, ASQUID can be a good platform for studying basic properties of quantum systems and motion sensing.

In the past decades, a number of ring-shaped traps have been realized based on magnetic and optical dipole trapping [9–13, 20], which paves the way for the creation of ASQUIDs. As sketched in Fig.1 a typical ASQUID is formed by confining Bose-Einstein condensate (BEC) in a ring-shaped trap. Potential barriers acting as Josephson junctions are created by blue-detuned laser beams. In Fig. 1 the two junctions are located at $\theta = 0$ and $\theta = \pi$, and they divide the ring-shaped trap into two re-

gions. The potential barriers can be set into motion to create particle number density bias or simulate the rotation of the system[6, 8]. ASQUIDs with single junction and double junctions have been constructed and studied in the cold-atom experiments, simulating the radio frequency (RF) SQUIDs and the direct current (DC) SQUIDs in the traditional electronics, respectively. In the setup with single junction the phase slips [4] and hysteresis [7] have been observed. In the one with double junctions the Josephson effect [5] and resistive flow [6] have been investigated, and interestingly the response of such a system subject to rotation was observed recently [8].

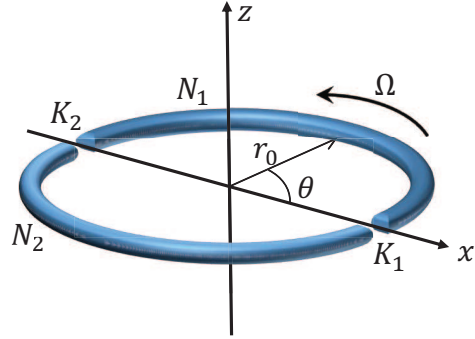


FIG. 1: (Color online) The sketch of the ASQUID with double junctions. The tunneling strength of the junctions are denoted by K_1 and K_2 . The particle numbers in the two regions are N_1 and N_2 . The ASQUID is rotating with an angular velocity Ω .

The usual theoretical analysis on the ASQUID is to directly implement the DC SQUID theory that was employed in the conventional SQUID, however, which is not a complete theory for the ASQUID. One of the major differences between the conventional SQUID and the ASQUID is that the conventional SQUID is connected

*Electronic address: boyangleo@gmail.com

to a battery, and hence a constant voltage drop can be maintained across the SQUID. The particle number bias in the SQUID is then a constant and a steady current through the SQUID can be derived. The ASQUID is an isolated system. In this case the particle numbers in each region vary with time. Hence, a theory suitable for the ASQUID has to be established. In this work we systematically construct a theory that describes the setup of ASQUID depicted in Fig. 1. Based on this theory we found two physical quantities that can be used for sensing the rotation, and we discussed how the variation of the Josephson junctions affects the motion sensing.

Our work is organized as the following. In Sec. II we construct a model for the setup in Fig. 1 using the tunneling Hamiltonian method, and based on which we obtain the differential equations that describe the dynamics of the system. In Sec. III we introduce a physical quantity that can be used for the rotation sensing, the critical population bias. We study the response of it to the rotation in case of symmetric junctions. In Sec. IV we study the behavior of the critical population bias in case of asymmetric junction. In Sec. V the case of dynamical Josephson junctions is investigated. Here, we introduce another physical quantity that can be used for the rotation sensing, namely, the critical time. Finally, Sec. VI provides our conclusions.

II. MODEL

We consider a model with BEC confined in a quasi-1D ring-shaped trap as sketched in Fig. 1. Using the tunneling Hamiltonian method the Hamiltonian of the system can be cast into three parts as the following

$$\hat{H} = \hat{H}_1 + \hat{H}_2 + H_t, \quad (1)$$

where

$$\begin{aligned} \hat{H}_1 &= \int_0^\pi d\theta r_0 \left(-\frac{\hbar^2}{2mr_0^2} \hat{\psi}_1^\dagger(\theta) \frac{\partial^2}{\partial \theta^2} \hat{\psi}_1(\theta) + U |\hat{\psi}_1(\theta)|^4 \right), \\ \hat{H}_2 &= \int_{-\pi}^0 d\theta r_0 \left(-\frac{\hbar^2}{2mr_0^2} \hat{\psi}_2^\dagger(\theta) \frac{\partial^2}{\partial \theta^2} \hat{\psi}_2(\theta) + U |\hat{\psi}_2(\theta)|^4 \right). \end{aligned} \quad (2)$$

Hamiltonian \hat{H}_i ($i = 1, 2$) describes the BECs in the i -th region, and $\hat{\psi}_i^\dagger$ and $\hat{\psi}_i$ are the creation and annihilation operators of the bosons in these regions. U is the interaction strength of the bosons. The particle numbers for region 1 and 2 are N_1 and N_2 , respectively, and the total particle number $N = N_1 + N_2$ is fixed. The radius of the quasi-1D ring-shaped trap is r_0 . The part \hat{H}_t describes the particle tunneling between the two regions as the following

$$\begin{aligned} \hat{H}_t &= \int_{-\pi}^\pi d\theta r_0 \left\{ K_1 \delta(\theta) [\hat{\psi}_1^\dagger(\theta) \hat{\psi}_2(\theta) + \hat{\psi}_2^\dagger(\theta) \hat{\psi}_1(\theta)] \right. \\ &\quad \left. + K_2 \delta(\theta - \pi) [\hat{\psi}_1^\dagger(\theta) \hat{\psi}_2(\theta) + \hat{\psi}_2^\dagger(\theta) \hat{\psi}_1(\theta)] \right\}. \end{aligned} \quad (3)$$

H_t describes the tunneling of the bosons through the two Josephson junctions. The locations of the junctions are at $\theta = 0$ and π , and the tunneling strength are described by the parameters K_1 and K_2 , respectively.

Here we consider a rotating system, which can be simulated by the movement of the Josephson junctions in the realistic experiments. In the rotating frame the Hamiltonian is given by

$$H' = H - \Omega J_z, \quad (4)$$

where Ω is the angular velocity. We are dealing with a uniform rotating system in this work, hence, Ω is a constant. $J_z = -i\hbar \frac{\partial}{\partial \theta}$ is the angular momentum operator in \hat{z} direction. When the tunneling between the BECs in the two regions is turned off, the ground states are supercurrent states, which carry angular momenta. The macroscopic wave functions of these states can be written as $\psi_i = \sqrt{n_i} e^{i(m_i \theta + \alpha_i)}$, ($i = 1, 2$). n_i is the number densities, and the phases of condensates are linearly dependent on the angle θ . When there is no tunneling, the parameters n_i , m_i and α_i are all constants. When the tunneling is turned on, the system becomes dynamical. Since we only consider the case of weak link between the two condensates, we assume the form of the ground state wave function doesn't change except the parameters n_i , m_i and α_i become time dependent, which can be expressed as the following

$$\psi_i(\theta, t) = \sqrt{n_i(t)} e^{i(m_i(t)\theta + \alpha_i(t))}. \quad (5)$$

To study the dynamical properties we employ the action principle $\delta \int_{t_1}^{t_2} L dt = 0$, where the Lagrangian is cast as

$$L = \int_0^\pi d\theta r_0 \hat{\psi}_1^\dagger i \hbar \partial_t \hat{\psi}_1 + \int_{-\pi}^0 d\theta r_0 \hat{\psi}_2^\dagger i \hbar \partial_t \hat{\psi}_2 - H'. \quad (6)$$

In the mean-field level the Lagrangian can be calculated by replacing the field operators $\hat{\psi}_i$ with the ground state wave function in Eq. (5). Then the dynamical behaviors of system can be derived from the Euler-Lagrange equations $\frac{\partial L}{\partial \lambda} = \frac{\partial}{\partial t} \left(\frac{\partial L}{\partial \dot{\lambda}} \right)$, where $\dot{\lambda} = \partial_t \lambda$ and λ represents all the six parameters $n_i(t)$, $m_i(t)$ and $\alpha_i(t)$. Straight forward calculation yields

$$\begin{aligned} m_+ &= \frac{4\Omega}{\Omega_0} + \frac{8K_2}{\hbar\Omega_0\sqrt{1-Z^2}} \sin\left(\Phi + \frac{m_+}{2}\pi\right) + \frac{2\pi\partial_t Z}{\Omega_0(1-Z^2)}, \\ m_- &= -\frac{8K_2 Z}{\hbar\Omega_0\sqrt{1-Z^2}} \sin\left(\Phi + \frac{m_+}{2}\pi\right) - \frac{2\pi Z \partial_t Z}{\Omega_0(1-Z^2)}, \\ \partial_t \Phi &= -\frac{\Omega_0 m_-}{4} \left(m_+ - \frac{4\Omega}{\Omega_0} \right) - \frac{2\tilde{U}Z}{\hbar} \\ &\quad + \frac{2Z}{\pi\hbar\sqrt{1-Z^2}} \left[K_+ \cos\Phi \cos\left(\frac{m_+}{2}\pi\right) + K_- \sin\Phi \sin\left(\frac{m_+}{2}\pi\right) \right], \\ \partial_t Z &= \\ &\quad - \frac{2}{\pi\hbar} \sqrt{1-Z^2} \left[K_+ \sin\Phi \cos\left(\frac{m_+}{2}\pi\right) - K_- \cos\Phi \sin\left(\frac{m_+}{2}\pi\right) \right]. \end{aligned} \quad (7)$$

In above equations we redefine some of the parameters as $m_{\pm}(t) = m_1(t) \pm m_2(t)$, $K_{\pm} = K_1 \pm K_2$, and $\Phi = \alpha_1(t) - \alpha_2(t) + \pi m_+ / 2$. The population bias between the two region is defined as $Z(t) = (N_1(t) - N_2(t)) / N$. The interaction strength is redefined as $\tilde{U} = UN / \pi r_0$. In the ring trap the flow of the superfluid is quantized, that is, the phase of the wave function winds up by $2\pi n$ along the ring trap, where n is an integer. Then, the flow circulation can be calculated as $\kappa = nh/m$ [21]. The circulation with a unit winding number is h/m . Correspondingly, we can define a fundamental rotation rate

$$\Omega_0 = h/mA, \quad (8)$$

where $A = \pi r_0^2$ is the area of the ring trap. Basically, Ω_0 can be taken as the angular velocity of the superfluid. Furthermore, we can also set a fundamental energy scale for the system, that is, the kinetic energy per atom of the superfluid with circulation h/m . It can be calculated as $E_0 = \frac{1}{2} m r_0^2 \Omega_0^2 = \hbar \Omega_0$. In this work E_0 will be used as the unit of energy.

As we have discussed previously, one of the differences between the conventional SQUID and the ASQUID is that ASQUID is an isolated system and the particle number bias $Z(t)$ varies with time. However, the result of the conventional SQUID can be treated as a special case of above model, that is, it can be reduced from Eqs. (7) with some assumptions. The current through the ASQUID can be calculated as $I \equiv \frac{1}{2} \frac{\partial}{\partial t} (N_1 - N_2) = \frac{N}{2} \frac{\partial Z(t)}{\partial t}$. In order to derive the result of the conventional SQUID, we assume very weak links, $K_1 = K_2 \ll \hbar \Omega$, and the two regions will not be charged up, that is, we set the terms of $\partial Z / \partial t$ in equations of m_{\pm} to zeros. Then, it's straightforward to derive the current from the forth equation in Eqs. (7) as the following

$$I = I_c \sin \Phi, \quad (9)$$

where $I_c \simeq \frac{N K_{\pm}}{\pi \hbar} \cos(2\pi \Omega / \Omega_0)$. This is exactly the result of a superfluid quantum interference device [22]. It's also in the same form as the current of a conventional SQUID, except that the $\cos(2\pi \Omega / \Omega_0)$ part should be replaced by $\cos(e\Phi / \hbar)$ in the case of SQUID since the SQUID is coupled to the magnetic field [23], where Φ is the magnetic flux through the SQUID.

III. THE CRITICAL POPULATION BIAS FOR SYMMETRIC JOSEPHSON JUNCTIONS

The conventional SQUID measures the magnetic field by reading the rapid oscillating Josephson current. However, it's difficult to directly observe the Josephson current in ASQUIDs since the ASQUID is an isolated system. Hence, new physical quantities that respond to the rotation has to be found. In this work we find that the critical population bias Z_c demonstrates a periodic modulation behavior due to the rotation. The critical population bias Z_c is the initial population bias where the

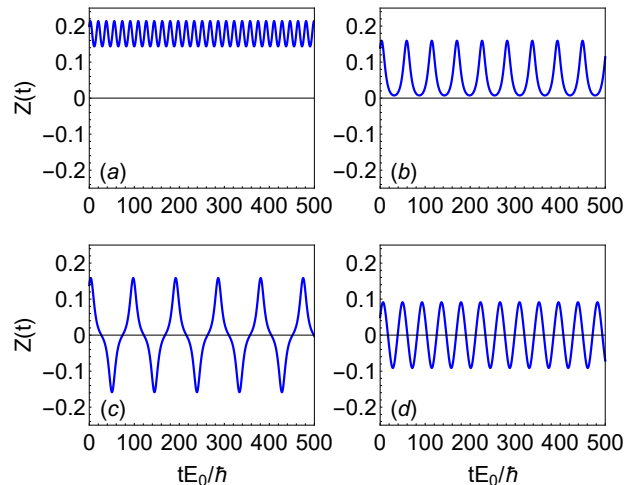


FIG. 2: (Color online) The temporal variation of the population bias $Z(t)$ for different initial values. (a), $Z(0) = 0.2$; (b), $Z(0) = 0.14$; (c), $Z(0) = 0.139$; (d), $Z(0) = 0.05$. The initial phase $\Phi(0) = 1$, $\Omega / \Omega_0 = 0.5$, $K_1 / E_0 = K_2 / E_0 = 0.01$, $\tilde{U} / E_0 = 1$ for all the graphs.

system switches between the self-trapping regime and the Josephson oscillation regime [15]. In Fig. 2 we demonstrate the variation of the population bias $Z(t)$ for different initial values $Z(0)$. For large initial values $Z(0)$ the system shows a behavior of self-trapping as illustrated in Fig. 2 (a), while for small $Z(0)$ system shows a behavior of Josephson oscillation as shown in Fig. 2 (d). The critical value Z_c for the transition between the self-trapping and the Josephson oscillation is found at the turning point with certain precision. For instance, when the initial population bias is set to $Z(0) = 0.14$ the system is in self-trapping regime as shown in Fig. 2 (b). When the initial population bias slightly decreases to $Z(0) = 0.139$ the system enters the Josephson oscillation regime as shown in Fig. 2 (c). Then the critical population bias is taken as $Z_c = 0.139$.

In this section we will focus on the case of symmetric junctions, that is, $K_1 = K_2$. We find that the critical population bias Z_c demonstrates a periodic modulation due to the variation of the angular velocity Ω of the rotation as shown in Fig. 3. Different curves are corresponding to different initial phase difference $\Phi(0)$. For a fixed phase difference $\Phi(0)$ and Ω there are two critical population bias with opposite signs since the two reservoirs are symmetric. The periodic modulation of Z_c clearly demonstrate that it can be used to measure the angular velocity of the rotation. The distance between the two adjacent peaks is $\Omega_0 / 2$, so the sensitivity of the measurement is determined by the quantity of Ω_0 . From Eq. (8) one observes that the sensitivity can be improved by increasing the ring trap radius r_0 . In the experiment of Ref. [8] the fundamental rotation rate Ω_0 is measured. Their definition of Ω_0 is different from ours by a factor of 2. To compare their measurement with our calculations the measured value must be multiplied by 2. After do-

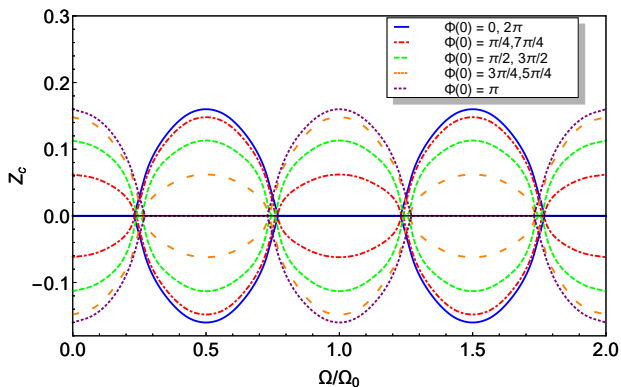


FIG. 3: (Color online) The critical population bias Z_c as a function of Ω/Ω_0 for different initial phases $\Phi(0)$. $K_1/E_0 = K_2/E_0 = 0.01$, $\tilde{U}/E_0 = 1$ for all the curves.

ing that the measured value is roughly $\Omega_0 \approx 72\text{Hz}$ for the case of $r_0 = 4.82\mu\text{m}$ [8]. Using Eq.(8) the Ω_0 is calculated as $\Omega_0 = 62.6\text{Hz}$, which is close to the measured value.

In cold atom physics the initial phases of the condensates are controllable and can be easily determined by phase imprinting techniques [16–20]. The choice of the initial phase difference $\Phi(0)$ is also important for the measurement of rotation. In Fig. 3 one observes that the curves of $\Phi(0) = 0$, or π are totally flat in some regions. For these curves the sensitivity of the measurement of rotation is low since there are no peak structures in some regions. On the other hand, the initial phase close to $\pi/2$ or $3\pi/2$ is better choice for the measurement since they show clear peak structures in all the region.

IV. THE CRITICAL POPULATION BIAS FOR ASYMMETRIC JOSEPHSON JUNCTIONS

In cold atom experiments, the Josephson Junctions are created by blue-detuned laser beams, and hence the tunneling strength K_1 and K_2 can be easily tuned by changing the intensity of the laser beams[4, 12]. In this section we investigate the effects of the asymmetry of the two junctions, that is, the case of $K_1 \neq K_2$. In Fig. 4 (a) we set $K_1 = 0.01E_0$ and $\Phi(0) = \pi/2$, and plot the critical population bias Z_c for different values of K_2 , which varies from $0.01E_0$ to $0.001E_0$. When $K_2 = K_1$ the curves show an oscillating behavior with period of $\Omega = 0.5\Omega_0$. When K_2 decreases, the positive and negative branches of the curves start separating from each other and a gap is opened at the points of $\Omega = (n+0.75)\Omega_0$, ($n = 0, \pm 1, \pm 2, \dots$). When K_2 is smaller than K_1 by one order of magnitude, the period of the curves becomes $\Omega = \Omega_0$. In Fig.4 (a) we set $K_2 = 0.01E_0$ and $\Phi(0) = \pi/2$, and plot Z_c for different values of K_1 . The curves shows similar behaviors except that the positive and negative branches separated from each other at points of $\Omega = (n + 0.25)\Omega_0$, ($n = 0, \pm 1, \pm 2, \dots$). From above observations we can conclude that the symmetric

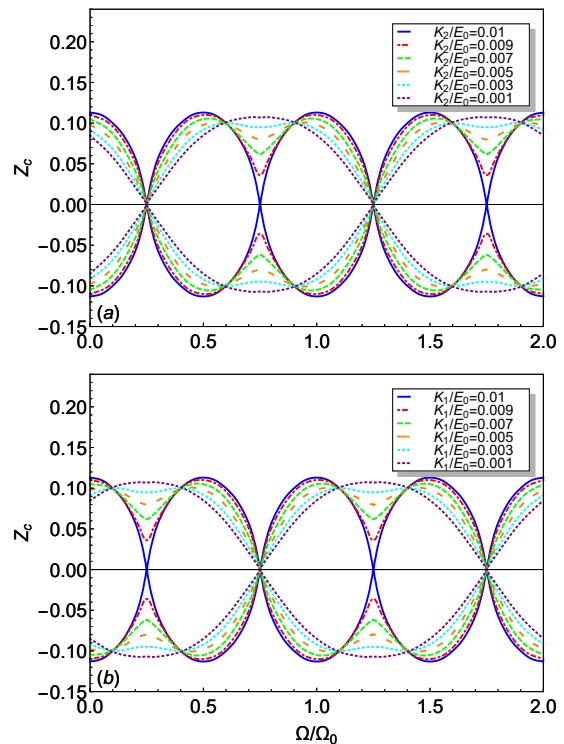


FIG. 4: (Color online) The critical population bias Z_c as a function of Ω/Ω_0 . In (a) K_1/E_0 is fixed at 0.01, while K_2/E_0 decreases from 0.01 to 0.001 for different curves. In (b) K_2/E_0 is fixed at 0.01, while K_1/E_0 decreases from 0.01 to 0.001 for different curves. The initial phase $\Phi(0) = \pi/2$ and $\tilde{U}/E_0 = 1$ for all the graphs.

junctions are better choice for the rotation sensing since the asymmetry of the junctions can blur two adjacent peaks. When K_1 and K_2 are different by a order of magnitude, two peaks merge into one. Hence, the sensitivity is lowered.

V. THE ROTATION MEASUREMENT FOR DYNAMICAL JOSEPHSON JUNCTIONS

In this section we explore another physical quantity that responds to the rotation. As we have discussed in the previous section, the strength of the Josephson junctions can be easily tuned by changing the intensity of the laser beams. Here we consider dynamical Josephson junctions, that is, time dependent K_1 and K_2 . For simplicity we take identical Josephson junctions and assume that they increase linearly with respect to time as $K_1(t) = K_2(t) = \alpha t$, where the parameter α is very small so that the changing of the system is an adiabatic process. The system is in the self-trapping regime initially since K_1 and K_2 are very small. As K_1 and K_2 increase to certain value the system changes from the self-trapping regime to the Josephson oscillation regime. Here we take the moment when $Z(t)$ reaches 0 to characterize the tran-

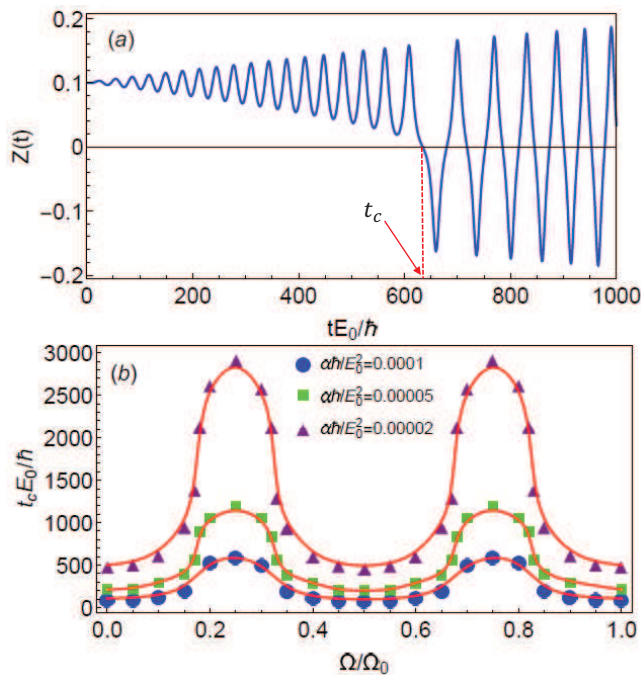


FIG. 5: (Color online) (a) The temporal variation of the population bias $Z(t)$ when the tunneling strength adiabatically changes as $K_1(t) = K_2(t) = \alpha t$, where $\alpha\hbar/E_0^2 = 10^{-5}$. (b) The critical time t_c as a function of Ω/Ω_0 for different values of α . Blue dots, green squares and brown triangles are for $\alpha\hbar/E_0^2 = 10^{-4}$, $\alpha\hbar/E_0^2 = 5 \times 10^{-5}$ and $\alpha\hbar/E_0^2 = 2 \times 10^{-5}$, respectively. The red solid lines are fitted by the method of cubic spline interpolation. The initial phase $\Phi(0) = \pi/2$ and $\tilde{U}/E_0 = 1$ for all the graphs.

sition as show in Fig. 5 (a). We call it the critical time t_c . In 5 (b) we plot the variation of the critical time t_c with respect to the angular velocity Ω and find that t_c also has a periodic modulation behavior. The period is $\Omega = 0.5\Omega_0$, which is the same as the one of the critical population bias Z_c . Compared with the critical population bias the measurement of the critical time is an easier way to detect the rotation since the critical time can be find in one procedure of the experiment, while one has

to take the experiment many times with different initial population bias $Z(0)$ to find the critical population bias Z_c .

VI. CONCLUSIONS

In summary, we establish an analytic model for the ASQUID with two tunable junctions using tunneling Hamiltonian method. Based on this model we found two physical quantities that can be used for rotation sensing, the critical population bias Z_c and the critical time t_c . We discussed the variation of Z_c for two cases. First, when the junctions are symmetric, that is, $K_1 = K_2$, Z_c demonstrates behavior of period modulation. The distance between two adjacent peaks is $\Omega_0/2$. Hence, the sensitivity of the ASQUID as a rotation sensor is determined by Ω_0 . In our model $\Omega_0 = h/m\pi r_0^2$, hence the sensitivity is eventually determined by the mass of the atoms and the radius r_0 of the ring trap. Second, when the junctions are asymmetric, that is, $K_1 \neq K_2$, we find that the asymmetry can lead to blurriness of the two adjacent peaks and thus lower the sensitivity. Finally we discussed the case of dynamic junctions, namely, the parameters K_1 and K_2 are time dependent. When K_1 and K_2 are adiabatically increasing the system can change from the self-trapping regime to the Josephson oscillation regime. The time of the transition is called the critical time t_c , which also demonstrates a behavior of periodic modulation due to the rotation. These investigations enrich the toolbox of motion sensing in cold atom physics.

Furthermore, the model and method we established in this work can be easily extended to more complicated systems, for instance, the ASQUIDs with spinor BECs or spin-orbit coupled superfluids, where we can explore more ways to detect the rotation.

VII. ACKNOWLEDGEMENTS

The work is supported by the National Science Foundation of China (Grant No. NSFC-11874002).

-
- [1] L. Amico, M. Boshier, G. Birkl, et al, AVS Quantum Sci. **3**, 039201 (2021).
 - [2] L. Amico, D. Anderson, M. Boshier, J.-P. Brantut, L.-C. Kwek, A. Minguzzi, and W. von Klitzing, Rev. Mod. Phys. **94**, 041001 (2022).
 - [3] J. Clarke and A. I. Braginski, *The SQUID Handbook* (Wiley-VCH, Weinheim, 2004), Vols. 1-2.
 - [4] K. C. Wright, R. B. Blakestad, C. J. Lobb, W. D. Phillips, and G. K. Campbell, Phys. Rev. Lett. **110**, 025302 (2013).
 - [5] C. Ryu, P.W. Blackburn, A. A. Blinova, and M. G. Boshier, Phys. Rev. Lett. **111**, 205301 (2013)
 - [6] F. Jendrzejewski, S. Eckel, N. Murray, C. Lanier, M. Edwards, C. J. Lobb, and G. K. Campbell, Phys. Rev. Lett. **113**, 045305 (2014).
 - [7] S. Eckel, J. G. Lee, F. Jendrzejewski, N. Murray, C. W. Clark, C. J. Lobb, W. D. Phillips, M. Edwards, and G. K. Campbell, Nature **506**, 200 (2014).
 - [8] C. Ryu, E. C. Samson, and M. G. Boshier, Nature Communications **11**, 3338 (2020).
 - [9] S. Gupta, K. W. Murch, K. L. Moore, T. P. Purdy, and D. M. Stamper-Kurn, Phys. Rev. Lett. **95**, 143201 (2005).
 - [10] A. S. Arnold, C. S. Garvie, and E. Riis, Phys. Rev. A **73**, 041606 (2006).
 - [11] C. Ryu, M. F. Andersen, P. Cladé, V. Natarajan, K. Helmerson, and W. D. Phillips, Phys. Rev. Lett. **99**,

- 260401 (2007).
- [12] A. Ramanathan, K. Wright, S. R. Muniz, M. Zelan, W. Hill III, C. Lobb, K. Helmerson, W. Phillips, and G. Campbell, *Phys. Rev. Lett.* **106**, 130401 (2011).
- [13] Y. Cai, D. G. Allman, P. Sabharwal, and K. C. Wright, *Phys. Rev. Lett.* **128**, 150401 (2022).
- [14] G. D. Pace, K. Xhani, A. Muzi Falconi, M. Fedrizzi, N. Grani, D. H. Rajkov, M. Inguscio, F. Scazza, W. J. Kwon, and G. Roati, *Phys. Rev. X* **12**, 041037 (2022).
- [15] A. Smerzi, S. Fantoni, S. Giovanazzi, and S. R. Shenoy *Phys. Rev. Lett.* **79**, 4950 (1997).
- [16] Y. Zheng and J. Javanainen, Classical and Quantum Models for Phase Imprinting, *Phys. Rev. A* **67**, 035602 (2003).
- [17] T. Yefsah, A. T. Sommer, M. J. Ku, L. W. Cheuk, W. Ji, W. S. Bakr, and M. W. Zwierlein, *Nature (London)* **499**, 426 (2013).
- [18] A. Kumar, R. Dubessy, T. Badr, C. De Rossi, M. de G er de Herve, L. Longchambon, and H. Perrin, *Phys. Rev. A* **97**, 043615 (2018).
- [19] N. Luick, L. Sobirey, M. Bohlen, V. P. Singh, L. Mathey, T. Lompe, and H. Moritz, *Science* **369**, 89 (2020).
- [20] G. Del Pace, K. Xhani, A. Muzi Falconi, M. Fedrizzi, N. Grani, D. Hernandez Rajkov, M. Inguscio, F. Scazza, W. J. Kwon, and G. Roati, *Phys. Rev. X* **12**, 041037 (2022).
- [21] J. F. Annett, *Superconductivity, Superfluids and Condensates*, Oxford Master Series in Condensed Matter Physics, Oxford, (2004).
- [22] R. W. Simmonds, A. Marchenkov, E. Hoskinson, J. C. Davis, and R. E. Packard, *Nature* **412**, 55 (2001).
- [23] R. P. Feynman, R. B. Leighton, and M. Sands, *The Feynman lectures on physics. 3: Quantum mechanics*, Addison-Wesley Publishing Co., Inc., Reading, Mass, London (1965).